

Existence of photon region for stationary axisymmetric black holes

Prasad Padhye*¹, Kajol Paithankar^{† 2,3}, and Sanved Kolekar^{‡ 2}

¹Indian Institute of Science Education & Research (IISER), Mohali,
India

²Indian Institute of Astrophysics, Koramangala II Block, Bangalore
560034, India

³Pondicherry University, R.V. Nagar, Kalapet 605014, Puducherry, India

December 18, 2024

Abstract

The black hole shadow is fundamentally connected to the structure of light rings and photon region in the background geometry. We investigate spherical photon orbits (SPOs) and photon regions in generic asymptotically flat, stationary, axisymmetric black hole spacetimes. We formally define the photon region's boundary purely in terms of the background metric functions, independent of the photon's parameters like energy or angular momentum, and establish the existence of at least one photon region for such spacetimes. We further analyze its common features including overlap with the ergoregion and rotation sense of SPOs. Additionally, light rings are identified at the extrema of the photon region boundary curves in the (r, θ) plane. Our approach is validated against a few exact black hole solutions. Implications are discussed.

1 Introduction

The radio-imaging of the silhouette of the supermassive black holes M87* and Sgr A* released by Event Horizon Telescope (EHT) collaboration [1, 2] have opened up new avenues of probing strong field regimes and testing modified theories of gravity. Investigations of photon trajectories around black hole geometries and accretion physics play a

*ms18085@iisermohali.ac.in

†kajol.paithankar@iiap.res.in

‡sanved.kolekar@iiap.res.in

key role in such studies. In the former, comprehensive exploration of light rings, photon region, and their projection effects are significant in understanding how the black hole shadow appears to a distant observer for various black hole solutions in different gravity theories. For a review of such studies, see [3–8].

The black hole shadow and its boundary corresponding to the extent of the central dark patch is essentially related to unstable null geodesics spiraling outwards from perturbed spherical photon orbits (SPOs). For spherically symmetric black holes, it is relatively straightforward to examine their photon spheres, whereas for rotating black holes, one needs to analyze both the light rings as well as the whole photon region wherein the SPOs are confined to lie. The photon region and its structure are crucial for determining the features of a black hole shadow. Though the structure of the shadow depends on the observer’s position and motion in addition to the black hole’s parameters, the photon region itself is characterized entirely by the black hole’s geometry and depends only on the background spacetime metric.

The photon region and light rings (LRs) of the Kerr black hole have been elaborately described in the literature [9, 10]. The two LRs outside the horizon, one counter-rotating and one co-rotating with the black hole, are situated at the intersection of the boundary of the photon region with the equatorial plane [11]. For the Kerr-Newman-NUT black holes with a cosmological constant and the accelerated black holes of the Plebański–Demiański class, the analytical estimation of the photon region and the shadow can be found in [12, 13]. LRs have been extensively investigated in the spacetimes of exact black hole solutions as well as in generic backgrounds of spherically symmetric and stationary axisymmetric black holes and horizon-less ultra-compact objects. Based on the analysis of LRs around Kerr and Kerr-like black holes, the asymmetries of LRs have been obtained as a measure of violation of the no-hair theorem [14] in the latter case. In the backgrounds of rotating boson stars and Kerr black holes with scalar hair, the presence of a stable LR leads to trapped or quasi-bound orbits [15]. For a stationary axisymmetric horizon-less ultra-compact object, the LRs have been shown to occur in pairs, one at a saddle point and the other at a local extremum of the effective potential. One of the LRs is stable if the object is a solution of the Einstein field equations, which leads to nonlinear instabilities of the background spacetime [16]. If the ultra-compact object possesses an ergoregion, then at least one of its LRs lies outside the ergoregion [17]. In the case of stationary black holes, at least one LR occurs at a saddle point of the effective potential termed as a standard LR [18]. Assuming the outer LR of the ultra-compact object to be standard, the stability of the inner LR has been proved in any theory of gravity [19]. The existence of LRs causes invariant structures in the phase space that are related to the black hole shadow [20].

Although the existence of the light rings has been well-established in stationary axisymmetric spacetimes, a similar thorough inspection for the photon region is lacking. Photon regions have been mostly explored for exact black hole solutions with explicitly known metric functions. Given the exact black hole metric, the usual analytical method to derive the SPOs and the photon region in a 4-dimensional stationary axisymmetric

geometry is to identify the four constants of motion and then deduce the completely integrable form of null geodesic equations [11]. In asymptotically flat spacetime, the conserved energy, angular momentum, and the Hamiltonian of a photon are three trivial constants, while the fourth constant is typically obtained through the separation of the radial (r) and polar (θ) coordinates using the Hamilton-Jacobi equation. In cases where the metric functions are not defined or the separation of variables is not feasible, it becomes difficult to evaluate the SPOs and photon region analytically following the conventional method. In the present work, we circumvent this issue and examine the photon region in a generic stationary, axisymmetric black hole spacetime having a Killing horizon with the metric functions satisfying natural constraints. Using the form of the metric functions at the Killing horizon and the asymptotic flat boundary, we prove that at least one photon region exists in such spacetimes and further infer features of the photon regions that are common to all such stationary axisymmetric black hole spacetimes. The proof utilizes the effective potential $V(r, \theta)$ approach adapted for probing the light rings around stationary axisymmetric ultra-compact objects [16].

We first set up the background asymptotically flat stationary axisymmetric spacetime in section 2. We then describe the usual method taken in the literature so far towards analysing SPOs, photon region and then introduce a different approach in section 3. The construction of the photon region's boundary based on the effective potential $V(r, \theta)$ is given in section 3.1. This construction depends on the photon's parameters, namely the energy E and angular momentum L of a photon. Since the photon region is expected to be characterized only by the black hole's geometry, we reformulate the photon region boundary entirely in terms of the metric functions of the background spacetime in section 3.2. We then prove in section 3.3 that such a boundary and hence the photon region always exist in any stationary axisymmetric black hole spacetimes described by the metric in section 2 and further investigate salient features of these boundaries in section 4. We analyze the intersection of the photon region with the ergoregion in section 4.1, the rotation sense of SPOs in section 4.2, and light rings in section 4.3. We find that the boundary of the photon region closer to the horizon called the inner boundary, may lie partially inside and partially outside the ergoregion, and the SPOs traversing it are co-rotating with the black hole. Whereas the boundary away from the horizon, termed the outer boundary, always lies outside the ergoregion, and the SPOs traversing the outer boundary are counter-rotating. Further, the light rings on the boundaries are located at the extrema of the curves $r(\theta)$ defining the boundaries of the photon region. As a consistency check, we implement our approach to known cases of exact black hole solutions for which the photon region has been studied using the conventional method in section 5. The discussion is presented in section 6.

The metric signature adopted is $(-, +, +, +)$ and natural units $G = \hbar = c = 1$ are used.

2 Stationary axisymmetric black hole metric

We consider the most general 4-dimensional stationary axisymmetric black hole spacetime in Boyer-Lindquist-type coordinates (t, r, θ, ϕ) described by the metric [21],

$$ds^2 = g_{tt} dt^2 + 2g_{t\phi} dt d\phi + g_{\phi\phi} d\phi^2 + g_{rr} dr^2 + g_{\theta\theta} d\theta^2 \quad (2.1)$$

where, the metric coefficients g_{ij} are smooth continuously differentiable functions of coordinates r and θ and are independent of t and ϕ . The metric is thus adapted to the killing vectors, ∂_t and ∂_ϕ corresponding to the isometries of stationarity and axisymmetry. The convention for the rotation sense of the black hole is such that $g_{t\phi} < 0$. Further, the black hole geometry has an event horizon at $r = r_H$ such that $g^{rr}(r_H, \theta) = 0$ and a stationary limit surface (SLS) at $r = r_g$ such that $g_{tt}(r_g, \theta) = 0$. Our region of interest is the domain of outer communication $r > r_H$, where r_H is the outermost event horizon. As per the signature adopted, the metric coefficients g_{rr} , $g_{\theta\theta}$ and $g_{\phi\phi}$ are positive everywhere outside the horizon, whereas the coefficient g_{tt} is positive between the horizon and the SLS. Beyond the SLS, for $r > r_g$, we have $g_{tt} < 0$. The ergoregion lies between the outermost event horizon and the SLS, with $g_{tt} > 0$ and $g_{rr} > 0$ in this region. The spacetime considered is assumed to be asymptotically flat, thus reducing it to the standard Minkowski metric form in spherical coordinates (t, r, θ, ϕ) at spatial infinity, with the metric functions simplifying to

$$g_{tt} \rightarrow -1, \quad g_{t\phi} \rightarrow 0, \quad g_{\phi\phi} \rightarrow r^2 \sin^2 \theta, \quad g_{rr} \rightarrow 1, \quad g_{\theta\theta} \rightarrow r^2 \quad (2.2)$$

Since we do not make any assumptions regarding the field equations, the results are valid in any metric theory of gravity wherein photons follow the null geodesics. For such black hole spacetimes, the Hamiltonian for null geodesics can be expressed as [16],

$$\begin{aligned} H &= g^{rr} (p_r)^2 + g^{\theta\theta} (p_\theta)^2 + g^{tt} (p_t)^2 + 2g^{t\phi} (p_t p_\phi) + g^{\phi\phi} (p_\phi)^2 \\ &= K(r, \theta) + V(r, \theta) \\ &= 0 \end{aligned} \quad (2.3)$$

where p_i is the null four-momentum vector. The kinetic term $K(r, \theta)$ and the potential term $V(r, \theta)$ are defined as,

$$K(r, \theta) = g^{rr} (p_r)^2 + g^{\theta\theta} (p_\theta)^2 \quad (2.4)$$

$$V(r, \theta) = g^{tt} (p_t)^2 + 2g^{t\phi} (p_t p_\phi) + g^{\phi\phi} (p_\phi)^2 \quad (2.5)$$

The potential $V(r, \theta)$ can also be expressed in terms of the covariant metric components g_{tt} , $g_{t\phi}$ and $g_{\phi\phi}$ using the conserved quantities derived from the symmetries of the spacetime. With the conserved quantities, namely the energy E and the angular momentum L of a photon, associated with the killing vectors ∂_t and ∂_ϕ , the potential term takes the form [16]

$$V = -\frac{1}{D} (g_{\phi\phi} E^2 + 2g_{t\phi} E L + g_{tt} L^2) \quad (2.6)$$

where $D = g_{t\phi}^2 - g_{tt}g_{\phi\phi}$ is the determinant of the 2-dimensional metric in (t, ϕ) space-time. We consider the determinant D to be non-zero everywhere outside the event horizon, thus enabling the existence of well-defined contravariant components of this 2-dimensional metric. One notes that, outside the horizon, at the SLS, $g_{tt} = 0$, implying $D > 0$ and thus constraining the determinant D to be positive everywhere outside the event horizon. Furthermore, we assume the event horizon to be a Killing horizon with the metric functions following $g_{t\phi}^2 - g_{tt}g_{\phi\phi} = 0$ at the horizon r_H [18]. In the black hole spacetimes, we then have $D > 0$ outside the event horizon and $D = 0$ on the null hypersurface of the black hole horizon.

3 Existence of the photon region

The standard definition of the photon region is the region in a black hole spacetime comprised of all (unstable and stable) spherical photon orbits (SPOs) having a constant radial coordinate r [12, 13, 20]. The set of photon geodesics parametrically very close to the unstable SPOs spiral outward, forming the image of the black hole shadow as seen by a distant observer. These SPOs may exist over a finite interval of radial coordinate r given by, say, $r_{in} \leq r \leq r_{out}$ and each SPO, with a fixed r , may oscillate between the limiting values, say θ_{min} and θ_{max} of the polar coordinate θ , depending on the explicit solution of the stationary axisymmetric black hole. A subset of these SPOs includes the orbits of the Killing vector $(\partial_t + \alpha \partial_\phi)$ called the light rings [16].

The photon region is reduced to a photon sphere in the case of a non-rotating spherically symmetric black hole. In rotating black hole spacetimes, the degeneracy between the co-rotating and counter-rotating photon orbits is lifted due to the frame-dragging effects. This results in the formation of a photon region with an inner boundary close to the horizon given by, say, $r_i(\theta)$ and an outer boundary given by $r_o(\theta)$ with $r_i(\theta) < r_o(\theta)$ for all θ .

We now briefly describe the conventional method followed in the literature to analytically probe the SPOs and the photon region and then emphasize the necessity of a generalized approach. In a stationary black hole spacetime, the Hamiltonian $H = 0$, the conserved energy E , and angular momentum L of a photon are standard constants for the photon's geodesics. Incorporating these constants and the exact functional form of the metric components, the Hamilton-Jacobi equation, $H(x, \partial S / \partial x) = 0$ (here x stands for (t, r, θ, ϕ)) is solved assuming the ansatz $S = S_t(t) + S_\phi(\phi) + S_r(r) + S_\theta(\theta)$ [11]. In particular spacetimes, this may lead to the separation of radial and polar coupled equations with an additional constant that appears as the separation constant. In the Kerr spacetime, this separation constant is Carter's constant [9]. In all the cases of known exact black hole solutions for which the SPOs and the black hole shadow have been explored analytically [12, 13], a Carter-like constant has been identified first. With the separate equations for r and θ coordinates, the definition of SPOs is sufficient to locate the photon region. In the cases wherein the separability cannot be determined or a Carter-like constant is not known, one can still evaluate the SPOs numerically using the

coupled set of equations on a case-by-case basis by choosing a set of initial conditions. However, this approach may be limited by the selection of initial conditions, and hence, the entire photon region, along with its true boundary, may not be recovered.

Consequently, our current understanding of photon region is restricted to the exact known black hole solutions with the caveats highlighted above. We, therefore, need a technique that helps in examining common features of the photon region in any stationary axisymmetric black hole spacetime admitting the SPOs. We illustrate such a technique that is independent of any constants of null geodesic motion and which utilizes only basic features of the metric functions describing the black holes' geometry.

In the following sections, we establish the equations defining the boundary of the photon region and demonstrate that the boundary and, hence, the photon region exists in all stationary axisymmetric black hole spacetimes described in section 2.

3.1 Photon region: formulation

In a stationary axisymmetric spacetime defined in the previous section, the motion of a photon in the (t, ϕ) dimensions is governed by

$$\dot{t} = \frac{g_{t\phi}L + g_{\phi\phi}E}{D} \quad (3.1)$$

$$\dot{\phi} = -\frac{g_{t\phi}E + g_{tt}L}{D} \quad (3.2)$$

where E and L are the photon's energy and angular momentum, as measured by an asymptotic static observer, and the dot represents the derivative with respect to an affine parameter. Since all the metric components g_{ij} depend on r and θ , the photon has only two degrees of freedom. The motion along r and θ then forms the kinetic part of the Hamiltonian with $K(r, \theta) \geq 0$. The potential part then follows $V(r, \theta) \leq 0$ from Eq.(2.3). This limits a photon's motion to the region in (r, θ) space where $V(r, \theta) \leq 0$. For each photon, in addition to the above equations for motion in the (t, ϕ) dimensions, there exist r and θ components of geodesic equations that are generally coupled equations.

We define the photon region as a collection of all spacetime events outside the outer horizon such that at least one SPO passes through an event in the set. The SPOs comprising the photon region are null geodesics on a constant r hypersurface, which by definition requires $\dot{r} = 0$ and $\ddot{r} = 0$. Further, a SPO in the photon region, though at fixed r , can have motion in the θ direction. We define the boundary of a photon region in the (r, θ) plane to be such that every point on the boundary is a turning point in θ , that is $\dot{\theta} = 0$, for at least one SPO passing through that point. The inner boundary of the photon region is then the collection of all such turning points (r, θ) , which forms a continuous and smooth curve $r_i(\theta)$ of the least possible value of r for each value of θ . A similar description will hold for the outer boundary $r_o(\theta)$ but with the maximum possible value of r for each θ . By this definition, the photons will have $\dot{\theta} = 0$ in addition to $\dot{r} = 0$ and $\ddot{r} = 0$ at the boundary of the photon region. We now reformulate these three conditions in two constraints on the potential $V(r, \theta)$ in the following way.

Imposing the conditions $\dot{r} = \dot{\theta} = 0$, that is $p_r = p_\theta = 0$, we get the kinetic term $K(r, \theta) = 0$ which further implies the potential $V(r, \theta) = 0$ at the boundary. Hence, the conditions $\dot{\theta} = 0$ and $V(r, \theta) = 0$ are equivalent for a SPO on the photon region boundary. The remaining condition $\ddot{r} = 0$ with $\dot{r} = 0$ translates to

$$\dot{p}_r = g_{rr}\ddot{r} + \dot{r}^2\partial_r g_{rr} = 0 \quad (3.3)$$

Then Hamilton's equation [16]

$$\dot{p}_r = -[(p_r)^2\partial_r g^{rr} + (p_\theta)^2\partial_r g^{\theta\theta} + \partial_r V(r, \theta)] \quad (3.4)$$

implies $\partial_r V(r, \theta) = 0$ at the boundary. A boundary of the photon region is, therefore, a curve $r_b(\theta)$ which simultaneously solves the following constraints on the potential:

$$V(r, \theta) = 0 \quad (3.5)$$

$$\partial_r V(r, \theta) = 0 \quad (3.6)$$

The photon region is then simply the region enclosed by the curves $r_b(\theta)$. Here, we would like to highlight that this construction of the photon region doesn't require a Carter-like constant at any step of the calculations. The above constraints on the potential imply that a photon traversing through a point, say $(r_b(\theta), \theta)$ on the photon region's boundary, encounters a potential $V(r_b, \theta) = 0$ which is also a local radial extremum (minimum or maximum along r) of the potential, satisfying $\partial_r V(r_b, \theta) = 0$.

Here, one would like to recall the definition of light rings as the orbits of the timelike killing vector $\partial_t + \alpha\partial_\phi$. Light rings are obtained as the solutions, say $\{r_L, \theta_L\}$ to the following constraints on the potential [16]:

$$V(r, \theta) = 0, \quad \partial_r V(r, \theta) = 0, \quad \partial_\theta V(r, \theta) = 0 \quad (3.7)$$

Thus, at the location of the light ring, the potential $V(r, \theta)$ is an extremum along both the coordinates r and θ . In the following subsection 4.3, we show that these light rings are located at the extrema of the boundary curves $r_i(\theta)$ and $r_o(\theta)$ of the inner and outer boundaries of the photon region.

3.2 Inner and Outer boundary of the photon region

The definition of photon region boundary given in terms of potential $V(r, \theta)$ has the shortcomings of depending on the photon's parameters E and L . We now eliminate these two parameters using the two constraint equations, Eq.(3.5) and (3.6) and define the photon region's boundary completely in terms of the metric functions g_{tt} , $g_{t\phi}$ and $g_{\phi\phi}$.

The potential $V(r, \theta)$ in Eq.(2.6) can be re-expressed as,

$$V(r, \theta) = -\frac{L^2}{D}(g_{\phi\phi}\sigma^2 + 2g_{t\phi}\sigma + g_{tt}) \quad (3.8)$$

where $\sigma = E/L$ and $D = g_{t\phi}^2 - g_{tt}g_{\phi\phi}$. Since D is non-zero outside the event horizon, a solution to the first constraint $V(r, \theta) = 0$ can be obtained as roots of the quadratic polynomial in σ . The two roots σ_{\pm} are given as

$$\sigma_{\pm} = \frac{-g_{t\phi} \pm \sqrt{(g_{t\phi})^2 - g_{\phi\phi}g_{tt}}}{g_{\phi\phi}} \quad (3.9)$$

With $g_{t\phi}$ taken to be negative, we can comment on the nature of these roots inside and outside the ergoregion. Within the ergoregion, $g_{tt} > 0$ implies that both σ_+ and σ_- are positive. Conversely, outside the ergoregion, $g_{tt} < 0$ results in a positive value for σ_+ and a negative value for σ_- . Here, one can note that, $\sigma_+ > \sigma_-$ regardless of the sign of $g_{t\phi}$. The roots σ_{\pm} determine the rotation sense of photons on SPOs (see section 4.2 for details). A photon with $\sigma > 0$ ($\sigma < 0$) travels on a co-rotating (counter-rotating) orbit. Now, considering the second constraint $\partial_r V(r, \theta) = 0$, we can write,

$$\partial_r V = -\frac{L^2}{D} (\partial_r g_{\phi\phi} \sigma^2 + 2 \partial_r g_{t\phi} \sigma + \partial_r g_{tt}) - (g_{\phi\phi} \sigma^2 + 2 g_{t\phi} \sigma + g_{tt}) \partial_r \left(\frac{L^2}{D} \right) = 0 \quad (3.10)$$

The second constraint equation is also a quadratic equation in σ and can be solved for two roots of the polynomial. However, it can be simplified further by considering that the photon region boundary is a simultaneous solution to the two constraints, Eq.(3.5) and (3.6). Imposing the first constraint $V(r, \theta) = 0$ results in reducing the second term in Eq.(3.10) to zero, thus simplifying it to,

$$(\partial_r g_{\phi\phi} \sigma^2 + 2 \partial_r g_{t\phi} \sigma + \partial_r g_{tt}) = 0 \quad (3.11)$$

Solving this equation for σ we get two roots $\bar{\sigma}_{\pm}$ as

$$\bar{\sigma}_{\pm} = \frac{-\partial_r g_{t\phi} \pm \sqrt{(\partial_r g_{t\phi})^2 - \partial_r g_{\phi\phi} \partial_r g_{tt}}}{\partial_r g_{\phi\phi}} \quad (3.12)$$

Since $\bar{\sigma}$ gives the ratio E/L for a photon orbiting a SPO, we expect it to be finite except near poles where $L \rightarrow 0$. For $\bar{\sigma}$ to be finite and real-valued, the metric components should satisfy $\partial_r g_{\phi\phi} > 0$ and $\partial_r g_{tt} < 0$. For further analysis, we assume that the black hole spacetimes follow $\partial_r g_{\phi\phi} > 0$ and $\partial_r g_{tt} < 0$. These conditions on the metric functions can be relaxed if one uses the H_+ and H_- potentials as defined for light rings in [16] and discussed more in section 3.3.

The solutions $\bar{\sigma}_+$ and $\bar{\sigma}_-$ are positive and negative, respectively, everywhere outside the horizon. However, unlike the σ_{\pm} solutions, one cannot comment on the rotation sense of photons based on the definition of the $\bar{\sigma}_{\pm}$ solutions. Hence, we need to find the correct pairs $\sigma_p = \bar{\sigma}_q$ that give the inner and outer boundary of the photon region. To note the nature (positivity/negativity) of these solutions inside and outside the ergoregion, we tabulate these cases below in Table 1.

	Inside ergoregion	Outside ergoregion
σ_+	positive	positive
σ_-	positive	negative
$\bar{\sigma}_+$	positive	positive
$\bar{\sigma}_-$	negative	negative

Table 1: σ and $\bar{\sigma}$ solutions inside and outside ergoregion

The SPO on the photon region boundary satisfies the two constraints Eqs. (3.5) and (3.6) simultaneously. Hence for such a SPO we have $E/L = \sigma_p = \bar{\sigma}_q$, where p and q could be $+$ or $-$. There are four possible pairs of σ_p and $\bar{\sigma}_q$. Two of the four pairs define the inner and outer boundary of the photon region, while the other two are physically invalid. Here, we note that in an axisymmetric spacetime as $g_{t\phi} \neq 0$, the roots σ_+ and σ_- can never be equal at any point (r, θ) outside the horizon. We now consider each $\bar{\sigma}_q$ root and, based on simple arguments, pair it with the appropriate σ_p root:

1. $\bar{\sigma}_-$: $\bar{\sigma}_-$ is negative everywhere outside the event horizon. Hence, in the case where $\bar{\sigma}_- = \sigma_p$, the photon moves on a counter-rotating orbit. Such an orbit can only exist outside the ergoregion. Hence, $\bar{\sigma}_-$ can only be paired with the σ_- solution outside the ergoregion, and the pair gives a boundary of the photon region that lies outside an ergoregion.
2. $\bar{\sigma}_+$: $\bar{\sigma}_+$ is positive outside the event horizon, and hence, in the case where $\bar{\sigma}_+ = \sigma_p$, the photon is moving on a co-rotating orbit. Therefore, $\bar{\sigma}_+$ cannot be paired with σ_- , as it will give a curve $r(\theta)$ that is discontinuous on the stationary limit surface. σ_+ is positive everywhere outside the event horizon, and hence, the second appropriate pair defining the photon region boundary is $\bar{\sigma}_+ = \sigma_+$.

The curve $r(\theta)$ obtained from $\bar{\sigma}_+ = \sigma_+$ may lie partially inside and partially outside the ergoregion, whereas the one obtained from $\bar{\sigma}_- = \sigma_-$ will lie completely outside the ergoregion. Thus, we can infer that $\bar{\sigma}_+ = \sigma_+$ leads to the inner boundary $r_i(\theta)$, while $\bar{\sigma}_- = \sigma_-$ leads to the outer boundary $r_o(\theta)$ of the photon region. Here, we emphasize that the inner and outer boundaries are obtained as solutions to the equations that depend only on the metric functions of background spacetime and are given as,

$$\left. \frac{-g_{t\phi} + \sqrt{(g_{t\phi})^2 - g_{\phi\phi}g_{tt}}}{g_{\phi\phi}} \right|_{r=r_i(\theta)} = \left. \frac{-\partial_r g_{t\phi} + \sqrt{(\partial_r g_{t\phi})^2 - \partial_r g_{\phi\phi} \partial_r g_{tt}}}{\partial_r g_{\phi\phi}} \right|_{r=r_i(\theta)} \quad (3.13)$$

$$\left. \frac{-g_{t\phi} - \sqrt{(g_{t\phi})^2 - g_{\phi\phi}g_{tt}}}{g_{\phi\phi}} \right|_{r=r_o(\theta)} = \left. \frac{-\partial_r g_{t\phi} - \sqrt{(\partial_r g_{t\phi})^2 - \partial_r g_{\phi\phi} \partial_r g_{tt}}}{\partial_r g_{\phi\phi}} \right|_{r=r_o(\theta)} \quad (3.14)$$

Following these definitions for inner and outer boundaries, we now prove in the next section that the boundaries and the photon region always exist in all stationary axisymmetric black hole spacetimes set up in section 2.

3.3 Existence of the photon region

To prove the existence of the photon region's boundaries, we first recall the approximations of metric functions near the Killing horizon given in [22]. The metric functions g_{tt} , $g_{t\phi}$ and $g_{\phi\phi}$ are related to the lapse function N and the frame dragging velocity ω through the following relations:

$$\omega = -\frac{g_{t\phi}}{g_{\phi\phi}} \quad \text{and} \quad N^2 = \omega^2 g_{\phi\phi} - g_{tt} \quad (3.15)$$

Based on the regularity of the the Ricci scalar \mathcal{R} and the traceless part of the Ricci tensor squared, $\mathcal{R}_{\mu\nu}\mathcal{R}^{\mu\nu} - \frac{1}{4}\mathcal{R}^2$, at the horizon, the lapse function N , the frame-dragging velocity ω and the metric coefficient $g_{\phi\phi}$ can be approximated as,

$$N(n, z) \simeq \kappa_H n + \mathcal{O}(n^3) \quad (3.16)$$

$$\omega(n, z) \simeq \omega_H + \frac{\omega_2(z) n^2}{2} + \mathcal{O}(n^3) \quad (3.17)$$

$$g_{\phi\phi}(n, z) \simeq g_{\phi\phi}^H(z) + \frac{g_{\phi\phi}^{(2)}(z) n^2}{2} + \mathcal{O}(n^3) \quad (3.18)$$

where n represents the normal distance to the horizon and z is the direction perpendicular to that of n . The constant κ_H is the surface gravity and is non-negative on the horizon. Further, $g_{\phi\phi} > 0$ and $\partial_r g_{\phi\phi} > 0$ translate to $g_{\phi\phi}^H > 0$ and $g_{\phi\phi}^{(2)} > 0$. Using these approximations and the relations in Eq.(3.15), we evaluate the roots σ_{\pm} and $\bar{\sigma}_{\pm}$ near the horizon. The leading-order terms for the roots are obtained as,

$$\sigma_+ = \omega_H + \left(\frac{\kappa_H}{\sqrt{g_{\phi\phi}^H}} \right) n + \mathcal{O}(n^2) \quad (3.19)$$

$$\sigma_- = \omega_H - \left(\frac{\kappa_H}{\sqrt{g_{\phi\phi}^H}} \right) n + \mathcal{O}(n^2) \quad (3.20)$$

$$\bar{\sigma}_+ = \omega_H + \frac{g_{\phi\phi}^H}{g_{\phi\phi}^{(2)}} \omega_2 + \sqrt{\frac{2(\kappa_H)^2}{g_{\phi\phi}^{(2)}} + \left(\frac{g_{\phi\phi}^H}{g_{\phi\phi}^{(2)}} \omega_2 \right)^2} + \mathcal{O}(n) \quad (3.21)$$

$$\bar{\sigma}_- = \omega_H + \frac{g_{\phi\phi}^H}{g_{\phi\phi}^{(2)}} \omega_2 - \sqrt{\frac{2(\kappa_H)^2}{g_{\phi\phi}^{(2)}} + \left(\frac{g_{\phi\phi}^H}{g_{\phi\phi}^{(2)}} \omega_2 \right)^2} + \mathcal{O}(n) \quad (3.22)$$

Under the assumption $g_{\phi\phi} > 0$ and $\partial_r g_{\phi\phi} > 0$, we get

$$\left| \frac{g_{\phi\phi}^H}{g_{\phi\phi}^{(2)}} \omega_2 \right| < \sqrt{\frac{2(\kappa_H)^2}{g_{\phi\phi}^{(2)}} + \left(\frac{g_{\phi\phi}^H}{g_{\phi\phi}^{(2)}} \omega_2 \right)^2} \quad (3.23)$$

Then in the limit $n \rightarrow 0$, we have,

$$\bar{\sigma}_+ > \omega_H \quad \text{and} \quad \bar{\sigma}_- < \omega_H \quad (3.24)$$

Thus, close to the horizon, the two pairs of roots satisfy

$$\bar{\sigma}_+ > \sigma_+ \quad \text{and} \quad \bar{\sigma}_- < \sigma_- \quad (3.25)$$

We now find such inequalities between the two pairs near spatial infinity. As the space-time is asymptotically flat, the metric functions near $r \rightarrow \infty$ can be approximated as [23]

$$g_{tt} \rightarrow -1 + \frac{C_1(\theta)}{r} + \mathcal{O}\left(\frac{1}{r^2}\right) \quad (3.26)$$

$$g_{t\phi} \rightarrow \frac{C_2(\theta)}{r} + \mathcal{O}\left(\frac{1}{r^2}\right) \quad (3.27)$$

$$g_{\phi\phi} \rightarrow r^2 \sin^2 \theta + \mathcal{O}\left(\frac{1}{r}\right) \quad (3.28)$$

Using these approximations in the definitions of σ_{\pm} and $\bar{\sigma}_{\pm}$, we get the asymptotic approximations of the four roots. The leading-order terms are given as,

$$\sigma_+ = \frac{1}{\sin \theta} \left(\frac{1}{r}\right) + \mathcal{O}\left(\frac{1}{r^3}\right) \quad (3.29)$$

$$\sigma_- = -\frac{1}{\sin \theta} \left(\frac{1}{r}\right) + \mathcal{O}\left(\frac{1}{r^3}\right) \quad (3.30)$$

$$\bar{\sigma}_+ = \frac{\sqrt{C_1(\theta)}}{\sqrt{2} \sin \theta} \left(\frac{1}{r^{3/2}}\right) + \mathcal{O}\left(\frac{1}{r^{5/2}}\right) \quad (3.31)$$

$$\bar{\sigma}_- = -\frac{\sqrt{C_1(\theta)}}{\sqrt{2} \sin \theta} \left(\frac{1}{r^{3/2}}\right) + \mathcal{O}\left(\frac{1}{r^{5/2}}\right) \quad (3.32)$$

Then, in $r \rightarrow \infty$ limit, we obtain the inequalities

$$\bar{\sigma}_+ < \sigma_+ \quad \text{and} \quad \bar{\sigma}_- > \sigma_- \quad (3.33)$$

A direct comparison between the relations in Eq.(3.25) and (3.33) leads to the following conclusion: Between the black hole horizon and the spatial infinity, there exist at least two curves $r_i(\theta)$ and $r_o(\theta)$ at which $\bar{\sigma}_+ = \sigma_+$ and $\bar{\sigma}_- = \sigma_-$ respectively. In other words, at least one inner boundary and one outer boundary of the photon region exist. Thus, at least one photon region exists in any stationary axisymmetric black hole spacetime described by the metric in section 2.

In the above discussion, we have assumed $\partial_r g_{\phi\phi} > 0$ and $\partial_r g_{tt} < 0$. However, these conditions on the metric functions can be relaxed if one uses the H_+ and H_- potentials defined for light rings in [16]. In that case, the definition of the photon region boundary

as given in Eqs. (3.5) and (3.6) in terms of the effective potential $V(r, \theta)$ translates to $\sigma = \sigma_+$ with $\partial_r \sigma_+ = 0$ for the co-rotating SPO at the inner boundary and $\sigma = \sigma_-$ with $\partial_r \sigma_- = 0$ for the counter-rotating SPO at the outer boundary. These will lead to the following relations on the metric functions

$$\frac{\left(g_{t\phi} - \sqrt{D}\right) \partial_r g_{\phi\phi} - g_{\phi\phi} \partial_r g_{t\phi}}{g_{\phi\phi}^2} + \frac{2g_{t\phi} \partial_r g_{t\phi} - \partial_r (g_{tt} g_{\phi\phi})}{2\sqrt{D} g_{\phi\phi}} = 0 \quad (3.34)$$

$$\frac{\left(g_{t\phi} + \sqrt{D}\right) \partial_r g_{\phi\phi} - g_{\phi\phi} \partial_r g_{t\phi}}{g_{\phi\phi}^2} - \frac{2g_{t\phi} \partial_r g_{t\phi} - \partial_r (g_{tt} g_{\phi\phi})}{2\sqrt{D} g_{\phi\phi}} = 0 \quad (3.35)$$

In the spacetimes, wherein $\partial_r g_{\phi\phi} > 0$ or $\partial_r g_{tt} < 0$ is not satisfied outside the outer horizon, one can use the above equations to obtain the photon region boundary. To prove the existence of a solution, a similar procedure can be followed by looking at the limits of the LHS in the above expressions near the horizon and at the spatial infinity to verify that they are of opposite signs and, hence, they are indeed equal to zero somewhere in the between.

4 General features of the photon region

Based on the definition of photon region given in section 3.2, we now explore some features such as overlapping of ergoregion and photon region, the rotation sense of the SPOs, and light rings located on the photon region boundary. These features are common to the photon regions of any stationary axisymmetric asymptotically flat black hole spacetime described in section 2.

4.1 Overlapping of photon region and ergoregion

We first determine the position of the boundaries with respect to the ergoregion. As per the definitions of inner and outer boundaries in section 3.2, the inner boundary of the photon region may lie partially inside and partially outside the ergoregion, whereas the outer boundary always lies outside the ergoregion. We revisit these arguments by examining the roots σ_{\pm} and $\bar{\sigma}_{\pm}$ at the SLS. At the SLS, $g_{tt}(r_g, \theta) = 0$ which implies

$$\sigma_+ = \frac{-g_{t\phi} + |g_{t\phi}|}{g_{\phi\phi}} = \frac{2|g_{t\phi}|}{g_{\phi\phi}} \quad (4.1)$$

$$\sigma_- = \frac{-g_{t\phi} - |g_{t\phi}|}{g_{\phi\phi}} = 0 \quad (4.2)$$

where $g_{t\phi} = -|g_{t\phi}|$ as $g_{t\phi}$ is assumed to be negative. Since the root $\bar{\sigma}_-$ is negative everywhere outside the event horizon (see table 1), at the SLS it follows,

$$\bar{\sigma}_-|_{r=r_g} < \sigma_-|_{r=r_g} \quad (4.3)$$

Comparing this inequality with the one in Eq.(3.33), we conclude that the curve $r_o(\theta)$ at which $\bar{\sigma}_- = \sigma_-$ lies between the SLS ($r = r_g$) and spatial infinity ($r \rightarrow \infty$). Thus, the outer boundary of the photon region lies outside the ergoregion. A similar discussion on the light rings in a stationary spacetime with an ergoregion can be found in [17].

The inner boundary of the photon region is given by the curve $r_i(\theta)$ at which $\bar{\sigma}_+ = \sigma_+$. If $\bar{\sigma}_+ > \sigma_+$ at the SLS, then the asymptotic relation in Eq.(3.33) implies that the curve $r_i(\theta)$ lies between the SLS and spatial infinity, that is, the inner boundary lies outside the ergoregion.

If there exists a point, say $(r_g(\theta_{in}), \theta_{in})$, where $\bar{\sigma}_+ = \sigma_+$ on the SLS, then the curve $r_i(\theta)$ intersects the SLS at this point and the inner boundary lies partially inside and partially outside the ergoregion. The point of intersection $(r_g(\theta_{in}), \theta_{in})$ can be evaluated using following condition:

$$\bar{\sigma}_+|_{r=r_g} = \sigma_+|_{r=r_g} = \frac{2|g_{t\phi}|}{g_{\phi\phi}} \quad (4.4)$$

4.2 Rotation sense of SPOs

We investigate the rotation sense of the photon orbits traversing the inner and outer boundaries of the photon region. The angular velocity of a photon with respect to a static asymptotic observer is given by the ratio $\Omega = \dot{\phi}/\dot{t}$. For a photon in the stationary axisymmetric set-up considered, we have

$$\dot{t} = \frac{g_{t\phi}L + g_{\phi\phi}E}{D} \quad (4.5)$$

$$\dot{\phi} = -\frac{g_{t\phi}E + g_{tt}L}{D} \quad (4.6)$$

which gives the angular velocity to be,

$$\Omega = -\frac{g_{t\phi}(E/L) + g_{tt}}{g_{t\phi} + g_{\phi\phi}(E/L)} \quad (4.7)$$

Further, the SPOs traversing the boundary of the photon region satisfy $V(r, \theta) = 0$, which is equivalent to,

$$g_{\phi\phi}\sigma^2 + 2g_{t\phi}\sigma + g_{tt} = 0 \quad (4.8)$$

with $\sigma = E/L$. This equation can be re-written as,

$$g_{t\phi}\sigma + g_{tt} = -\sigma(g_{\phi\phi}\sigma + g_{t\phi}) \quad (4.9)$$

Substituting this in Eq.(4.7) we get,

$$\Omega = \sigma \quad (4.10)$$

Thus, the rotation sense of the photon traversing the boundary of the photon region is determined by the ratio $\sigma = E/L$ of its conserved energy and angular momentum component. The Eq.(4.5), can be re-expressed as,

$$\frac{\dot{t}}{E} = \frac{g_{t\phi} + g_{\phi\phi}\sigma}{\sigma D} \quad (4.11)$$

On the inner boundary of the photon region, photons have $\sigma = \sigma_+$. Then using Eq.(3.9) we can write

$$\left. \frac{\dot{t}}{E} \right|_{\sigma=\sigma_+} = \frac{g_{t\phi} + g_{\phi\phi}\sigma_+}{\sigma_+ D} = \frac{+\sqrt{D}}{\sigma_+ D} = \frac{1}{\sigma_+ \sqrt{D}} \quad (4.12)$$

As σ_+ and D are positive everywhere outside the horizon, the quantity $\dot{t}/E > 0$ on the inner boundary. Since $\dot{t} > 0$ is a necessary condition for a physical photon, we have $E > 0$ on the inner boundary of the photon region. Similarly, using the definition of σ_- we can show that,

$$\left. \frac{\dot{t}}{E} \right|_{\sigma=\sigma_-} = \frac{g_{t\phi} + g_{\phi\phi}\sigma_-}{\sigma_- D} = \frac{-\sqrt{D}}{\sigma_- D} = \frac{-1}{\sigma_- \sqrt{D}} \quad (4.13)$$

As σ_- is negative and D is positive outside the ergoregion, the quantity $\dot{t}/E > 0$ and hence $E > 0$ on the outer boundary of the photon region.

Thus, from the viewpoint of an asymptotic observer, the photon trajectories traversing the outer boundary of the photon region have $\Omega = \sigma_- < 0$, that is, $L < 0$ and hence are counter-rotating. While the trajectories traversing the inner boundary with $\Omega = \sigma_+ > 0$ and hence $L > 0$ are co-rotating. This further confirms that the outer boundary lies outside the ergoregion as the counter-rotating trajectories can exist only outside the ergoregion. A similar analysis for the energy E and the rotation velocity Ω of photons moving on light rings in the equatorial plane can be found in [15].

4.3 Light rings

We show that the light rings are located at the extrema of the curves $r_i(\theta)$ and $r_o(\theta)$. Light rings are special cases of SPOs where the null geodesics are circular orbits confined to a fixed θ . Such circular orbits exist where the boundary of the photon region is tangent to the $r=\text{constant}$ hypersurface [12]. Consider the coordinate plane (r, θ) . The projection of $r=\text{constant}$ hypersurface in this plane is a $r=\text{constant}$ curve, and the projection of the photon region's boundaries are $r = r_i(\theta)$ and $r = r_o(\theta)$ curves. Since, at the position of light ring, say (r_L, θ_L) , the boundary of the photon region and the $r=\text{constant}$ hypersurface have a common tangent plane, the normal vectors η_μ , to these two hypersurfaces when projected in the (r, θ) plane should coincide at (r_L, θ_L) .

The $r=\text{constant}$ hypersurface has only one non-vanishing component η_r of the normal vector, whereas, for the boundaries of photon region, one can evaluate two components

η_r and η_θ . For the two normal vectors to coincide, the η_θ component should vanish at the position of a light ring. The η_θ component for the curves of the inner and the outer boundaries of the photon region can be obtained to be proportional to,

$$\eta_{\theta_i} \propto \frac{dr_i(\theta)}{d\theta} \quad \text{for inner boundary} \quad (4.14)$$

$$\eta_{\theta_o} \propto \frac{dr_o(\theta)}{d\theta} \quad \text{for outer boundary} \quad (4.15)$$

Hence, one can determine the coordinates of light rings as $(r_i(\theta_{L_i}), \theta_{L_i})$ on the inner boundary and $(r_o(\theta_{L_o}), \theta_{L_o})$ on the outer boundary where θ_{L_i} and θ_{L_o} are given by

$$\left. \frac{dr_i(\theta)}{d\theta} \right|_{\theta=\theta_{L_i}} = 0 \quad \text{and} \quad \left. \frac{dr_o(\theta)}{d\theta} \right|_{\theta=\theta_{L_o}} = 0 \quad (4.16)$$

The light rings are thus located at the extrema of the curves $r_i(\theta)$ and $r_o(\theta)$. Since light rings satisfy Eqs. (3.7) which involves one additional constraint $\partial_\theta V = 0$ compared to the definition of the photon region boundary, the extremum of $r_i(\theta)$ and $r_o(\theta)$ in the θ direction must be equivalent to $\ddot{\theta} = 0$ to maintain consistency with [16].

5 Implementation in different gravity theories

We now apply the definition of photon region and the features discussed in the previous sections to the cases of the Kerr and Kerr-Newman black hole solutions of Einstein's field equations and the Kerr-Sen black hole solution of heterotic string theory. These black hole solutions satisfy the conditions $g_{\phi\phi} > 0$, $\partial_r g_{tt} < 0$ and $\partial_r g_{\phi\phi} > 0$ outside the event horizon. For these black hole solutions, the photon region boundary has been evaluated using a Carter-like constant and separated radial and polar geodesic equations. Our technique to determine the photon region is shown to be consistent with these known solutions.

5.1 Kerr black hole

The metric for the Kerr black hole of mass m and spin parameter a in Boyer–Lindquist coordinates is given as,

$$ds^2 = - \left(1 - \frac{2mr}{\rho^2} \right) dt^2 + \frac{\rho^2}{\Delta} dr^2 + \rho^2 d\theta^2 - \frac{4mra \sin^2 \theta}{\rho^2} dt d\phi + \sin^2 \theta \left(r^2 + a^2 + \frac{2mra^2 \sin^2 \theta}{\rho^2} \right) d\phi^2 \quad (5.1)$$

where $\Delta = r^2 + a^2 - 2mr$ and $\rho^2 = r^2 + a^2 \cos^2 \theta$. The metric represents the Kerr black hole for $a \leq m$. The radii of the outer horizon r_H and the stationary limit surface r_g

are given by,

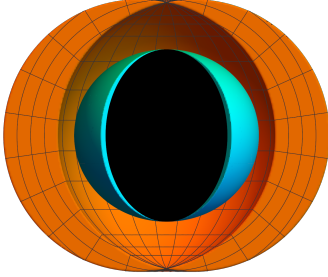
$$r_H = m + \sqrt{m^2 - a^2} \quad (5.2)$$

$$r_g = m + \sqrt{m^2 - a^2 \cos^2 \theta} \quad (5.3)$$

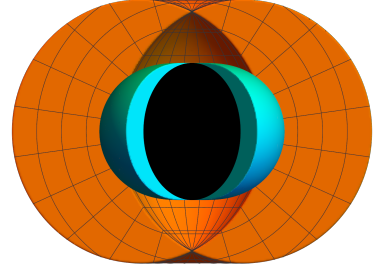
The separated equations for r and θ coordinates with Carter's constant results in an inequality representing the photon region, which is given as [11],

$$(\rho^2(r - m) - 2r\Delta)^2 \leq 4r^2\Delta a^2 \sin^2 \theta \quad (5.4)$$

Using this inequality, 3D illustrations of the photon region, the black hole horizon, and the ergoregion are plotted in Fig.1 for the two sets of black hole parameters $\{m, a\} = (4, 2)$ and $(4, 3.5)$.



(a) $m = 4, a = 2$



(b) $m = 4, a = 3.5$

Figure 1: 3D illustrations showing the photon region in orange, ergoregion in cyan, and the event horizon in black for Kerr black holes.

Now, using the Eqs. (3.13) and (3.14), the curves $r_i(\theta)$ and $r_o(\theta)$ corresponding to the inner and outer boundaries are plotted along with the stationary limit surface at $r_g(\theta)$ in Fig. 2. For comparison, the boundary curves $r_c(\theta)$ determined through the conventional way are also included in the same figure. The curves $r_c(\theta)$ satisfy

$$(\rho^2(r - m) - 2r\Delta)^2 = 4r^2\Delta a^2 \sin^2 \theta \quad (5.5)$$

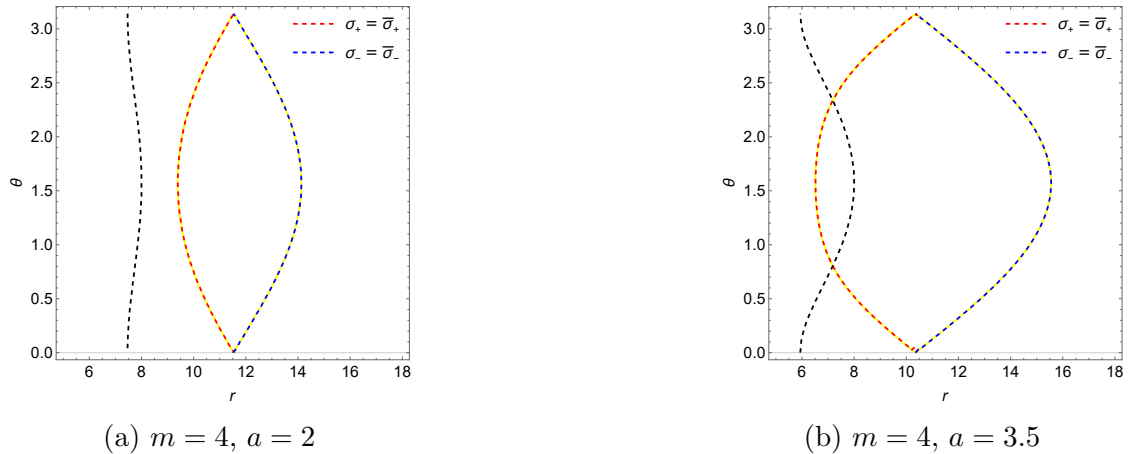


Figure 2: The red and blue dashed lines show the curves $r_i(\theta)$ and $r_o(\theta)$ of the inner and outer boundaries. The yellow line represents the curve $r_c(\theta)$. The black dashed lines show the stationary limit surface $r_g(\theta)$.

The overlapping of curves $r_i(\theta)$ and $r_o(\theta)$ with the curves $r_c(\theta)$ validates our technique. Further, the extrema of these curves lie in the equatorial plane, thus implying the existence of co-rotating and counter-rotating equatorial light rings [11].

The intersection of the inner boundary and the stationary limit surface is found by solving Eq.(4.4) for the intersection points $\{r_g(\theta_{in}), \theta_{in}\}$. For a fixed value of mass parameter m , the intersection points differ over the range of the spin parameter $a \leq m$. The intersection points θ_{in} are plotted over the range $a \leq m$ of the spin parameters in figure 3 below for $m = \{1, 1.5, 2\}$.

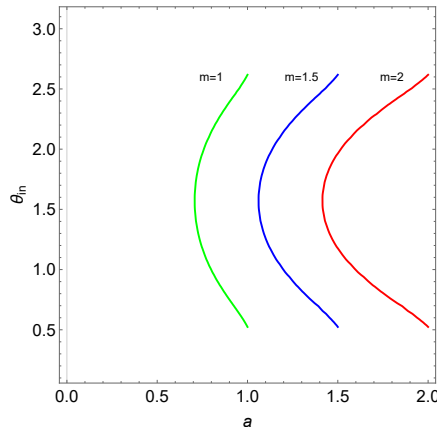


Figure 3: Intersection points θ_{in} for black hole mass $m = 1, 1.5$ and 2 and the spin parameter $a < m$

From the figure, one can note that corresponding to each mass parameter m , there exists a critical spin value, say a_c , beyond which the inner boundary of the photon region

doesn't intersect the stationary limit surface. Consequently, for a Kerr black hole of spin $a < a_c$, the inner boundary of the photon region lies completely outside the ergoregion. For $a > a_c$, there exists two intersection points θ_{in} for each spin a whereas at $a = a_c$, only one intersection point θ_{in} occurs at the equatorial plane with $\theta = \pi/2$. The critical spin a_c can be expressed as a function of mass m of the black hole and is given by [12],

$$a_c = \frac{m}{\sqrt{2}} \quad (5.6)$$

In the following subsections, we conduct a similar analysis for the Kerr-Newman and Kerr-Sen black holes. We find that, as in the case of the Kerr black hole, the boundary of the photon region obtained using the separated geodesic equations coincides with the one calculated using our technique for both black holes. Further, a critical spin value exists in both cases, beyond which the inner boundary of the photon region does not intersect the ergoregion and lies completely outside the ergoregion. The plots showing the intersection points and the expressions for critical spin parameters are presented for each of the black hole solutions in the corresponding subsections.

5.2 Kerr-Newman Black Hole

The Kerr-Newman black hole of mass M , spin a and charge Q in Boyer-Lindquist coordinates is given by [24]

$$ds^2 = - \left(1 - \frac{2Mr - Q^2}{\rho^2} \right) dt^2 + \frac{\rho^2}{\Delta} dr^2 + \rho^2 d\theta^2 - \frac{4Mr a \sin^2 \theta - 2aQ^2 \sin^2 \theta}{\rho^2} dt d\phi + \sin^2 \theta \left(\frac{(r^2 + a^2)^2 - \Delta a^2 \sin^2 \theta}{\rho^2} \right) d\phi^2 \quad (5.7)$$

where $\Delta = r^2 - 2Mr + a^2 + Q^2$ and $\rho^2 = r^2 + a^2 \cos^2 \theta$ and $M^2 \geq (Q^2 + a^2)$. The event horizon and the stationary limit surface are located at r_H and r_g and are given by

$$r_H = M + \sqrt{M^2 - Q^2 - a^2} \quad (5.8)$$

$$r_g(\theta) = M + \sqrt{M^2 - Q^2 - a^2 \cos^2 \theta} \quad (5.9)$$

Using the separated radial and polar geodesic equations in [24], the inequality describing the photon region can be evaluated to be,

$$(\eta_{KN} + a^2 \cos^2 \theta) \sin^2 \theta \geq \Phi_{KN}^2 \cos^2 \theta \quad (5.10)$$

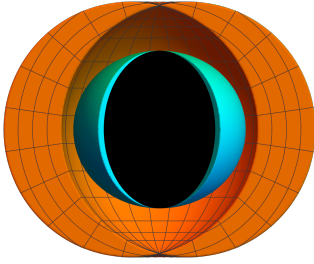
where

$$\eta_{KN} = - \frac{r^2 \left[4a^2 (Q^2 - Mr) + (r^2 - 3Mr + 2Q^2)^2 \right]}{a^2 (M - r)^2}$$

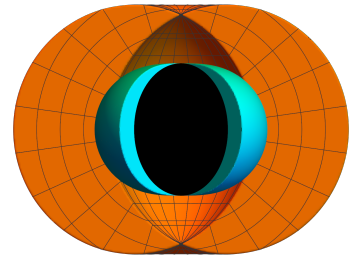
$$\Phi_{KN} = \frac{a^2 (M - r) + r (r^2 - 3Mr + 2Q^2)}{a (M - r)}$$

The photon region, ergoregion, and the black hole horizon are plotted in Fig 4 for black hole parameters $\{M, a, Q\} = \{4, 2, 2\}$ and $\{4, 3, 2\}$. Then, using the Eqs. (3.13) and (3.14), the inner boundary $r_i(\theta)$ and outer boundary $r_o(\theta)$ are plotted along with the stationary limit surface in Fig. 5. Additionally, the boundary $r_c(\theta)$ obtained using the separated radial and polar geodesic equations is also plotted in the same figure, which solves

$$(\eta_{KN} + a^2 \cos^2 \theta) \sin^2 \theta = \Phi_{KN}^2 \cos^2 \theta \quad (5.11)$$

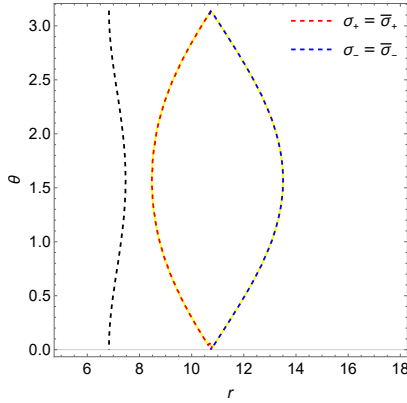


(a) $M = 4, a = 2, Q = 2$

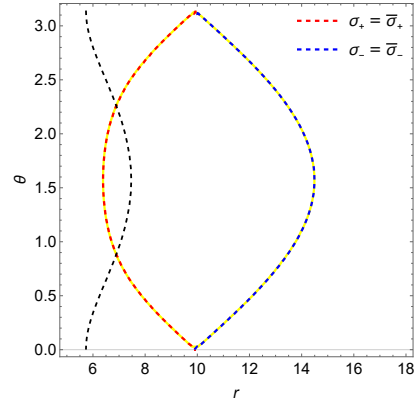


(b) $M = 4, a = 3, Q = 2$

Figure 4: 3D illustrations showing the photon region in orange, ergoregion in cyan, and the event horizon in black for Kerr-Newman black holes.



(a) $M = 4, a = 2, Q = 2$



(b) $M = 4, a = 3, Q = 2$

Figure 5: The red and blue dashed lines show the curves $r_i(\theta)$ and $r_o(\theta)$ of the inner and outer boundaries. The yellow line represents the curve $r_c(\theta)$. The black dashed lines show the stationary limit surface $r_g(\theta)$.

The curves $r_c(\theta)$ coincide with $r_i(\theta)$ and $r_o(\theta)$, which shows that our approach is consistent with the conventional method in the case of the Kerr-Newman black hole.

The intersection points θ_{in} of the inner boundary and the stationary limit surface are evaluated as solutions to the Eq.(4.4) and are plotted against the spin parameter over the range $a < \sqrt{M^2 - Q^2}$ for black holes of mass $M = \{4, 5, 6\}$ and charge $Q = \{2, 3\}$ in Fig. 6.

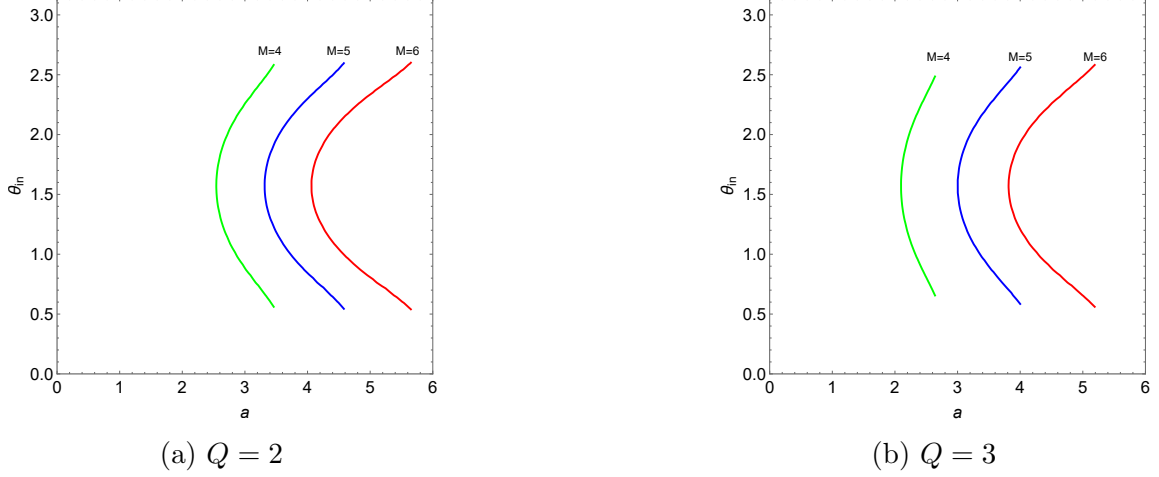


Figure 6: Intersection points θ_{in} for black hole mass $M = 4, 5, 6$ and the spin parameter $a < \sqrt{M^2 - Q^2}$

The critical spin at which the inner boundary intersects the stationary limit surface at the equatorial plane $\theta = \pi/2$ is derived as a function of mass M and charge Q of the black and is given by

$$a_c = \frac{\mathcal{A}_{M,Q} + \sqrt{2M R_g \mathcal{B}_{M,Q} - Q^2 \mathcal{H}_M(Q) \mathcal{H}_M(-Q)}}{4(Q^2 - 2MR_g) \sqrt{\mathcal{F}_{M,Q}}} \quad (5.12)$$

where

$$\begin{aligned} \mathcal{A}_{M,Q} &= Q^2 (40M^4 - 32M^2Q^2 + 3Q^4) - MR_g (80M^4 - 84M^2Q^2 + 17Q^4) \\ \mathcal{B}_{M,Q} &= (48M^4 - 44M^2Q^2 + 7Q^4) (48M^6 - 68M^4Q^2 + 23M^2Q^4 - Q^6) \\ \mathcal{F}_{M,Q} &= MR_g (16M^4 - 20M^2Q^2 + 5Q^4) - Q^2 (8M^4 - 8M^2Q^2 + Q^4) \\ \mathcal{H}_M(Q) &= 48M^5 - 24M^4Q - 44M^3Q^2 + 16M^2Q^3 + 7MQ^4 - Q^5 \end{aligned}$$

with $R_g = r_g(\theta = \pi/2) = M + \sqrt{M^2 - Q^2}$.

5.3 Kerr-Sen Black Hole

The line element of the Kerr-Sen black hole of mass M , spin a and charge Q in Boyer-Lindquist coordinates is [24, 25]

$$ds^2 = - \left(1 - \frac{2Mr}{\rho^2}\right) dt^2 + \rho^2 \left(\frac{dr^2}{\Delta} + d\theta^2\right) - \frac{4Mra \sin^2 \theta}{\rho^2} dt d\phi + \sin^2 \theta \left(r^2 + a^2 + \frac{Q^2 r}{M} + \frac{2Mra^2 \sin^2 \theta}{\rho^2}\right) d\phi^2 \quad (5.13)$$

where

$$\Delta = r^2 - 2Mr + a^2 + \frac{Q^2 r}{M} \quad (5.14)$$

$$\rho^2 = r^2 + a^2 \cos^2 \theta + \frac{Q^2 r}{M} \quad (5.15)$$

with $a < \sqrt{(M - Q^2/2M)^2}$. The radii of event horizon r_H and the stationary limit surface r_g are given by

$$r_H = M - \frac{Q^2}{2M} + \sqrt{\left(M - \frac{Q^2}{2M}\right)^2 - a^2} \quad (5.16)$$

$$r_g(\theta) = M - \frac{Q^2}{2M} + \sqrt{\left(M - \frac{Q^2}{2M}\right)^2 - a^2 \cos^2 \theta} \quad (5.17)$$

The inequality representing the photon region is deduced through the separated geodesic equations of radial and polar coordinates [24, 26] and is given as

$$(\eta_{KS} + a^2 \cos^2 \theta) \sin^2 \theta \geq \Phi_{KS}^2 \cos^2 \theta \quad (5.18)$$

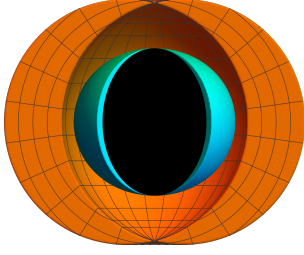
where

$$\eta_{KS} = - \frac{r^2 \left[(2M^2 (r^2 - 3Mr - Q^2) + 3MQ^2 r + Q^4)^2 - 8a^2 M^4 (2Mr + Q^2) \right]}{a^2 M^2 (2Mr - 2M^2 + Q^2)^2}$$

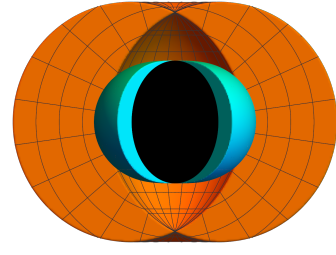
$$\Phi_{KS} = \frac{2a^2 M^2 (M + r) + a^2 M Q^2 - 6M^3 r^2 - 2M^2 Q^2 r + 2M^2 r^3 + 3M Q^2 r^2 + Q^4 r}{aM(2M^2 - 2Mr - Q^2)}$$

Using this inequality, the photon region, ergoregion, and the horizon are plotted below in Fig 7 for black hole parameters $\{M, a, Q\} = \{4, 2, 2\}$ and $\{4, 3, 2\}$. For the same set of black hole parameters, boundary curves $r_i(\theta)$ and $r_o(\theta)$ of the inner and outer boundaries are obtained using the Eqs. (3.13) and (3.14), along with the stationary limit surface in Fig. 8. The curves $r_c(\theta)$ of the boundaries deduced from the separated radial and polar geodesic equations are also plotted in the same figure. These curves satisfy

$$(\eta_{KS} + a^2 \cos^2 \theta) \sin^2 \theta = \Phi_{KS}^2 \cos^2 \theta \quad (5.19)$$

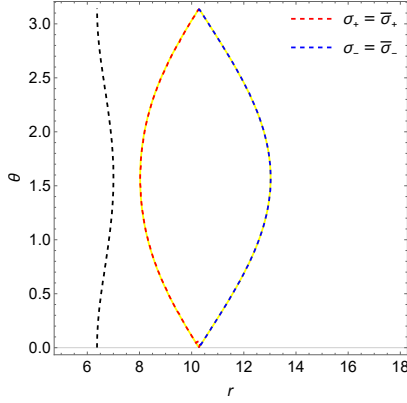


(a) $M = 4, a = 2, Q = 2$

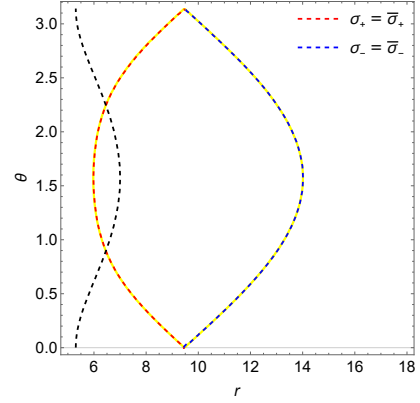


(b) $M = 4, a = 3, Q = 2$

Figure 7: 3D illustrations showing the photon region in orange, ergoregion in cyan, and the event horizon in black for Kerr-Sen black holes.



(a) $M = 4, a = 2, Q = 2$



(b) $m = 4, a = 3, Q = 2$

Figure 8: The red and blue dashed lines show the curves $r_i(\theta)$ and $r_o(\theta)$ of the inner and outer boundaries. The yellow line represents the curve $r_c(\theta)$. The black dashed lines show the stationary limit surface $r_g(\theta)$.

From the figure, one can note that the curves $r_c(\theta)$ overlap with the curves $r_i(\theta)$ and $r_o(\theta)$, thus proving the consistency of the two approaches for the Kerr-Sen black hole.

Further, the intersection of the inner boundary and the stationary limit surface at the points θ_{in} is plotted using Eq.(4.4) for black holes of mass $M = \{4, 5, 6\}$ and charges $Q = \{2, 3\}$ over the range $a < \sqrt{(M - Q^2/2M)^2}$ of the spin parameter in Fig. 9.

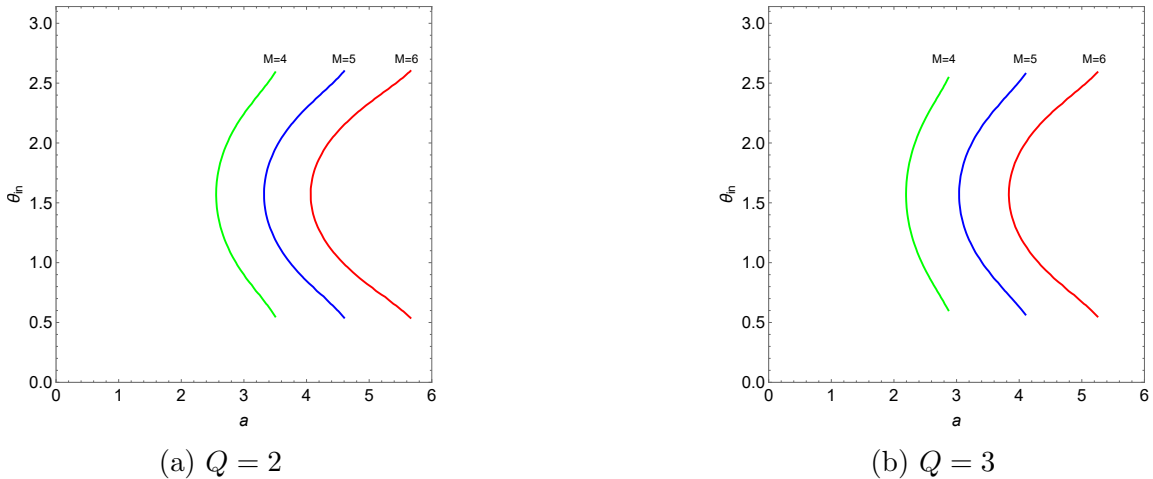


Figure 9: Intersection points θ_{in} for black hole mass $M = 4, 5, 6$ and the spin parameter $a < \sqrt{(M - Q^2/2M)^2}$

The critical spin corresponding to the single intersection point in the equatorial plane is derived as a function of mass M and charge Q of the black hole and is simply written as,

$$a_c = \frac{2M^2 - Q^2}{\sqrt{8M^2 - 2Q^2}} \quad (5.20)$$

6 Discussion

We provide a formal definition and establish a technique to construct the photon region boundaries and further prove that at least one photon region exists in general asymptotically flat, stationary axisymmetric black hole spacetimes. Notably, this approach does not rely on any constants of the photon's motion, and the photon region is entirely derived from the generic form of the background metric functions. The existence of the photon region is demonstrated by analyzing the behavior of the metric functions near the boundaries of the domain of outer communication, that is, the Killing horizon and the asymptotic spatial infinity. Since the metric functions are considered in a general form, all the results presented are applicable to asymptotically flat, stationary axisymmetric black holes in any theory of gravity that admits spherical photon orbits (SPOs).

Following this construct, some interesting features of the photon regions are identified, namely: The outer boundary of the photon region is always situated outside the ergoregion and is populated only by the counter-rotating photon orbits. Whereas the inner boundary is populated by co-rotating photon orbits. The photon region and the ergoregion overlap partially for a specific range of black hole parameters. In this range, the inner boundary of the photon region intersects the stationary limit surface. One can then expect limiting values of black hole parameters beyond which there is no overlap between the two regions. The black hole geometries with the limiting parameter values

(for example, the critical spin in section 5) are then likely to have only one common point between the photon region and the ergoregion in the (r, θ) plane.

Further, light rings are found to be located at the extrema along the polar angular direction of the curves $r_i(\theta)$ and $r_o(\theta)$ representing the inner and outer boundaries of the photon region respectively. This finding supports the presence of at least two light rings: one co-rotating light ring on the inner boundary and one counter-rotating light ring on the outer boundary of the photon region, which is consistent with the results of [18].

For horizon-less ultra-compact objects, the light rings are shown to occur in pairs for each rotation sense [16]. Then, by extending the current understanding of light rings on the photon region boundaries to ultra-compact objects, one can speculate the existence of multiple photon regions in such spacetimes, which would be interesting to investigate further.

References

- [1] Event Horizon Telescope Collaboration et al, ApJL, **875**, L1, (2019)
- [2] Event Horizon Telescope Collaboration et al, ApJL **930**, L12, (2022)
- [3] L. Amarilla and E. F. Eiroa, Phys. Rev. D **85**, 064019 (2012).
- [4] A. Abdujabbarov, M. Amir, B. Ahmedov, and S. G. Ghosh, Phys. Rev. D **93**, 104004 (2016).
- [5] Arne Grenzebach, *The Shadow of Black Holes-An Analytic Description* (Springer, Heidelberg, 2016).
- [6] P. V. P. Cunha, C. A. R. Herdeiro, B. Kleihaus, J. Kunz, and E. Radu, Phys. Lett. B **768**, 373 (2017).
- [7] T. Bronzwaer and H. Falcke, Astrophys. J. **920**, 155 (2021).
- [8] V. Perlick and O. Y. Tsupko, Phys. Rep. **947**, 1 (2022).
- [9] B. Carter, Phys. Rev. **174**, 1559 (1968).
- [10] E. Teo, Gen. Relativ. Gravit. **53**, 10 (2021).
- [11] V. Perlick, Black Holes, SS 2022, Universität Bremen, Germany.
- [12] A. Grenzebach, V. Perlick, and C. Lämmerzahl, Phys. Rev. D **89**, 124004 (2014).
- [13] A. Grenzebach, V. Perlick, and C. Lämmerzahl, Int. J. Mod. Phys. D **24**, 1542024 (2015).

- [14] T. Johannsen, *Astrophys. J.* **777**, 170 (2013).
- [15] P. V. P. Cunha, J. Grover, C. Herdeiro, E. Radu, H. Rúnarsson, and A. Wittig, *Phys. Rev. D* **94**, 104023 (2016).
- [16] P. V. P. Cunha, E. Berti, and C. A. R. Herdeiro, *Phys. Rev. Lett.* **119**, 251102 (2017).
- [17] R. Ghosh and S. Sarkar, *Phys. Rev. D* **104**, 044019 (2021).
- [18] Pedro V. P. Cunha and Carlos A. R. Herdeiro, *Phys. Rev. Lett.* **124**, 181101 (2020).
- [19] F. Di Filippo, *Phys. Rev. D* **110**, 084026 (2024).
- [20] J. Grover and A. Wittig, *Phys. Rev. D* **96**, 024045 (2017).
- [21] Subrahmanyan Chandrasekhar, *The Mathematical Theory of Black Holes* (Oxford University Press, 1983).
- [22] A. J. M. Medved, Damien Martin, and Matt Visser, *Phys. Rev. D* **70**, 024009 (2004).
- [23] D. Astefanesei, R. B. Mann, and C. Stelea, *Phys. Rev. D* **75**, 024007 (2007).
- [24] Sérgio Vinicius M. C. B. Xavier, Pedro V. P. Cunha, Luís C. B. Crispino, and Carlos A. R. Herdeiro, *Int. J. Mod. Phys. D* **29**, 2041005 (2020).
- [25] A. Sen, *Phys. Rev. Lett.* **69**, 1006 (1992).
- [26] Rashmi Uniyal, Hemwati Nandan, and K. D. Purohit, *Classical Quantum Gravity* **35**, 025003 (2018).